# Crystal structure of a 1,6-bis(phenylethynyl)pyrene-based cyclophane that exhibits mechanochromic luminescence



| | |
|---|---|
| Journal: | *Molecular Systems Design & Engineering* |
| Manuscript ID | ME-ART-09-2021-000131.R1 |
| Article Type: | Paper |
| Date Submitted by the Author: | 23-Sep-2021 |
| Complete List of Authors: | Simizu, Shohei; Tokyo Institute of Technology, Department of Materials Science and Engineering<br>Thazhathethil, Shakkeeb; Hokkaido University, Research Institute for Electronic Science; Tokyo Institute of Technology, Department of Materials Science and Engineering<br>Takahashi, Kiyonori; Hokkaido University, Research Institute for Electronic Science; Hokkaido University, Graduate School of Environmental Science<br>Nakamura, Takayoshi; Hokkaido University, Research Institute for Electronic Science<br>Sagara, Yoshimitsu; Tokyo Institute of Technology, Department of Materials Science and Engineering |
| | |

ARTICLE

# Crystal structure of a 1,6-bis(phenylethynyl)pyrene-based cyclophane that exhibits mechanochromic luminescence

Received 00th January 20xx,
Accepted 00th January 20xx

DOI: 10.1039/x0xx00000x

Shohei Shimizu,[a] Shakkeeb Thazhathethil,[a,b] Kiyonori Takahashi,*[b] Takayoshi Nakamura,[b] and Yoshimitsu Sagara*[a]

Cyclophanes featuring luminophores are considered promising candidates as thermal or mechanical stimuli-responsive luminescent materials. The mechanism of the changes in the photophysical properties on the crystal-crystal or crystal-amorphous phase transitions can be easily clarified, owing to the crystal structure of the cyclophanes. However, in the case where flexible aliphatic chains are introduced to the target cyclophane, the procurement of the crystals suitable for single-crystal X-ray analysis is challenging. Conversely, the introduction of significantly shorter linkers between large π-conjugated groups leads to difficulties in compound purification, resulting in incorrect photophysical properties, particularly in the solid state. Herein, we report the crystal structure of a 1,6-bis(phenylethynyl)pyrene-based cyclophane and mechanoresponsive luminescence. The cyclophane has a naphthalene group as another aromatic group, and the two different π-conjugated groups are bridged by tetraethylene glycol linkers. Single-crystal X-ray analysis revealed that the pyrene and naphthalene moieties form intramolecular π-stacked structures in the crystals, and intermolecular excimer formation of the luminophores was not observed. The arrangement of the isolated luminophore results in light-blue emission with a well-resolved vibronic structure in the fluorescence spectrum. Mechanical grinding induces a phase transition from crystal to amorphous, which was confirmed by the powder X-ray diffraction measurements, and the emission colour turns green. The photoluminescence spectroscopy and emission lifetime measurements clarified that the green emission is ascribed to intermolecular excimer formation. Subsequent thermal treatment recovers the initial light-blue-emissive crystalline state. The crystalline phase is thermodynamically stable, whereas the amorphous state is thermodynamically metastable.

**Design, System, Application**

To date, mechanoresponsive luminescence, exhibited by luminescent cyclophanes, has not been sufficiently explored; this is partially because solving or estimating the molecular assembled structures is difficult. Herein, a novel 1,6-bis(phenylethynyl)pyrene-based cyclophane was designed to have two tetraethylene glycol chains as the linkers between the luminophore and a naphthalene moiety. The moderately sized linkers allow access to single crystal structures, which are otherwise challenging owing to their flexible and cyclic structure. Similar to other previously reported luminescent cyclophanes, the proposed cyclophane exhibits mechanoresponsive luminescence. Because the molecular assembled structures were clarified, the correlation between the luminophore arrangement in the crystals and mechanoresponsive luminescence can be easily determined. Our molecular design strategy adopted in this study can also be applied to other luminophores, which could facilitate the development of a series of mechanochromic and/or thermochromic luminescent cyclophanes.

## Introduction

Numerous organic or organometallic compounds with various molecular structures have been reported to exhibit mechanoresponsive luminescence.[1-5] The mechanical or thermal stimuli-induced changes in the emission properties, caused by the rearrangement and/or conformational changes of the luminophores, are significantly evident in phase transitions from ordered-to-ordered or ordered-to-amorphous states. Most of the reported mechanoresponsive luminescence compounds are normally acyclic. Although limited examples have been reported,[6-11] the luminophores featuring cyclic structures, which tend to exhibit multiple thermodynamically stable and metastable states due to less sterically hindered molecular mobility, are expected to form molecular assemblies that more reliably change their photoluminescence colours through external stimuli, such as grinding or crushing, temperature change, or exposure to solvent vapours.[6-11]

[a] Department of Materials Science and Engineering, Tokyo Institute of Technology, 2-12-1, Ookayama, Meguro-ku, Tokyo 152-8552, Japan.
E-mail: sagara.y.aa@m.titech.ac.jp
[b] Research Institute for Electronic Science, Hokkaido University, N20, W10, Kita-ku, Sapporo, Hokkaido 001-0020, Japan.
E-mail: ktakahashi@es.hokudai.ac.jp

†Electronic Supplementary Information (ESI) available: Synthesis of compound **1**, crystallographic data, and additional Figures. See DOI: 10.1039/x0xx00000x

Cyclophanes comprise aromatic groups and aliphatic linkers bridging the aromatic moieties.[12-15] The cyclic structures work as hosts explored in supramolecular chemistry,[12,16-22] and can become a part of the interlocked supramolecular architectures.[23-34] In addition, several cyclophanes have been found to exhibit liquid-crystalline (LC) properties.[35-42] Incorporating luminophores to cyclophanes provides characteristic photophysical properties for the isolated state in solution.[43-48] The luminescent cyclophanes can function as chemosensors for guest molecules and ions.[49-58] They can also be regarded as potential candidates to achieve mechano- and/or thermoresponsive luminescence.[8-11,59-63] When two or more π-conjugated groups are introduced to a single cyclophane, a periodic, alternating, or sequential arrangement of aromatic groups can be achieved, which are preferable to induce external stimuli-induced emission colour changes in the molecular assembled states. Several cyclophanes containing luminophores with high quantum yields have been designed and explored for stimuli responsiveness in the course of our studies.[8-11,59-63] Luminescent cyclophanes containing hexaethylene glycol linkers bridging the aromatic groups provide different emission colours in the nematic LC phase compared to the other crystalline states.[9,10] Although the LC character allows us to access supercooled LC phases that can be utilised for reversible emission colour changes of triplet-triplet annihilation-based photon upconversion[61] or linearly polarised photoluminescence,[63] crystals suitable for single-crystal X-ray analysis have not been obtained due to the flexible nature inherent to the hexaethylene glycol linkers. In addition, when the volume of the planer-extended π-conjugated groups are relatively large in individual cyclophanes, the solubility for the organic solvents decreases and purification of the compound and single-crystal growth becomes more challenging.[11] To successfully determine the molecular packed cyclophane structures and correlate the luminophore arrangement with mechano- or thermoresponsive luminescence, the luminescent cyclophanes should be appropriately designed to mitigate these challenges and simplify the preparation of single crystals.

Recently, we successfully solved crystal structures of 9,10-bis(phenylethynyl)anthracene-based cyclophanes with either tetraethylene glycol or pentaethylene glycol linkers.[8,59] The cyclophane with tetraethylene glycol linkers was observed as two different crystalline forms.[8] One crystalline form exhibits a two-step mechanoresponsive luminescence, whereas the other releases guest solvent molecules upon grinding. However, luminescent cyclophanes, whose crystal structures are solved, are limited.

Herein, we report the crystal structure of 1,6-bis(phenylethynyl)pyrene-based cyclophane **1** (Fig. 1) and its mechanoresponsive luminescence. This particular luminophore was used because of its simple molecular structure and high fluorescence quantum yield.[64,65] Prior to cyclophane **1**, no other crystal structures containing 1,6-bis(phenylethynyl)pyrene have been reported. The powder-like crystalline form exhibits light-blue fluorescence. The grinding of cyclophane **1** converts the crystalline form to the amorphous state. This amorphous state exhibits green photoluminescence, which is ascribed to intramolecular excimers. Subsequent thermal treatment recrystallises the amorphous state back to the initial crystalline state that exhibits light-blue fluorescence. Cyclophane **1** was also found to show a nematic LC phase above 178.3 °C.

## Results and discussion

### Molecular design

The aromatic moieties in cyclophane **1** are 1,6-bis(phenylethynyl)pyrene and 1,5-disubstituted naphthalene (Fig. 1). The highly emissive character of 1,6-bis(phenylethynyl)pyrene[64,65] has been utilised for supramolecular fibres,[66,67] rotaxanes,[68] cyclophanes,[9,10,62] and mechanoresponsive luminescent materials.[69,70] The two π-conjugated groups in cyclophane **1** are bridged by two tetraethylene glycol chains. The linkers are shorter than those used in cyclophane **2** prepared in our previous study.[9] The nematic LC phase of cyclophane **2**, observed above 106.9 °C, exhibits a green emission ascribed to intermolecular excimer formation of the luminophores. Rapid cooling of **2** from the nematic phase results in a supercooled nematic LC phase at room temperature (r.t.), which retains its green emissive character. Subsequent annealing at 80 °C induces a phase transition to a crystalline phase that provides a blue emission colour.[9] Furthermore, the crystals show mechano-responsive luminescence. Because the linkers are longer, the structure of **2** is significantly flexible and well-ordered crystals suitable for single-crystal X-ray analysis could not be obtained. Cyclophane **1** was designed with tetraethylene glycols linkers, which are shorter and less flexible but still long enough to provide sufficient solubility in common organic solvents. Compound **3**, which is a synthetic intermediate of cyclophanes **1** and **2**, was also used as a monomer analogue in this study.

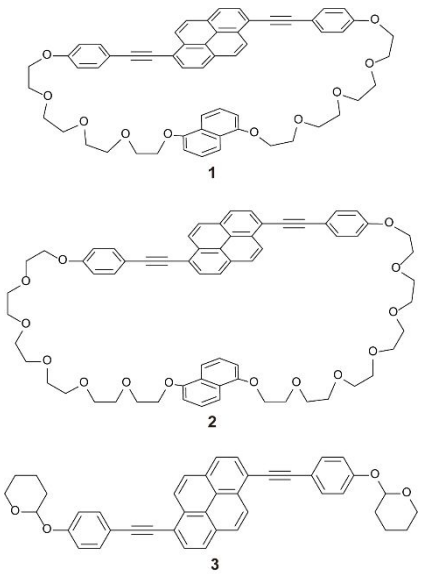


**Fig. 1** Molecular structures of 1,6-bis(phenylethynyl)pyrene-based cyclophane **1**, previously reported cyclophane **2**, and reference compound **3**.

Cyclophane **1** was prepared through a Williamson ether reaction between 1,6-bis(4-hydroxyphenylethynyl)pyrene and naphthalene with two bromo-terminated tetraethyleneglycol groups (see ESI†) and characterised by $^{1}$H NMR, $^{13}$C NMR, MALDI-TOF-MS spectra, and elemental analysis. The cyclic structure of **1** resulted in peak shifts in the $^{1}$H NMR spectra that correspond to the aromatic groups (Fig. 2). All peaks ascribed to the central pyrene moiety in the luminophore of **1** are shifted upfield compared to those of acyclic compound **3**. The unambiguous shifts indicated that the naphthalene group in **1** tends to be in the proximity of the luminophore due to its cyclic character. The $^{1}$H NMR spectrum obtained for compound **2** (Fig. 2c) suggested that the larger cycle reduces the effect because the two aromatic groups are separated for longer periods in solution. The peaks corresponding to the naphthalene moiety also show similar effects, whereas only slight shifts were observed for the peaks ascribed to the two outer phenylene groups of the luminophore.

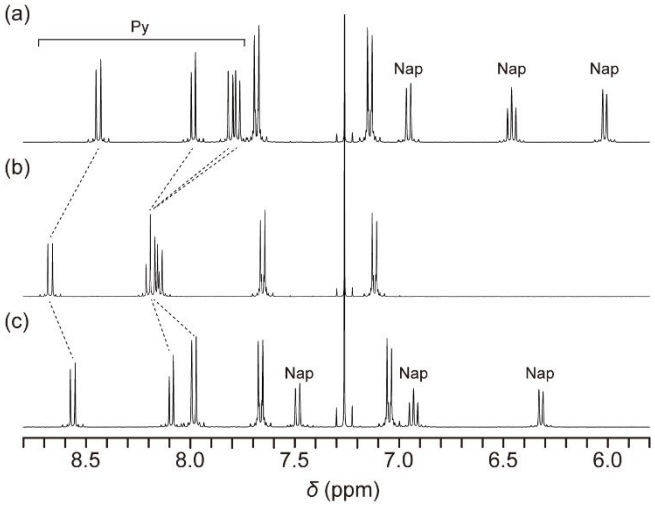


**Fig. 2** Partial $^{1}$H NMR spectra of (a) cyclophane **1**, (b) compound **3**, and (c) cyclophane **2** in $CDCl_3$ at r.t. The abbreviations "Py" and "Nap" indicate signals ascribed to the pyrene and naphthalene moieties, respectively.

### Crystal structure

The appropriate length of the tetraethylene glycol linkers in cyclophane **1** facilitated the growth of crystals suitable for single-crystal X-ray analysis. Recrystallisation from a mixture of diethyl ether and $CHCl_3$ yielded yellow crystals that exhibit light-blue emission. The crystal system and space group of **1** at –100 °C were triclinic and *P*-1, respectively (Table S1 and Fig. S1). The molecular structure of **1** in the crystal is shown in Fig. 3a. The pyrene and naphthalene rings in a single **1** molecule interact via intramolecular π•••π interactions, where the interplanar angle and the nearest carbon (C)•••C distances are 2.12° and 3.435 Å, respectively. The two phenylene rings bonded to pyrene via C≡C bonds are denoted as **phA** and **phB**, respectively. The interplanar angles between the **phA**•••pyrene and **phB**•••pyrene rings are 74.12° and 15.20°, respectively. It is noteworthy that a 9,10-bis(phenylethynyl)anthracene-based cyclophane having the same linkers and naphthalene moiety as cyclophane **1** forms different arrangements of aromatic groups in the crystals,

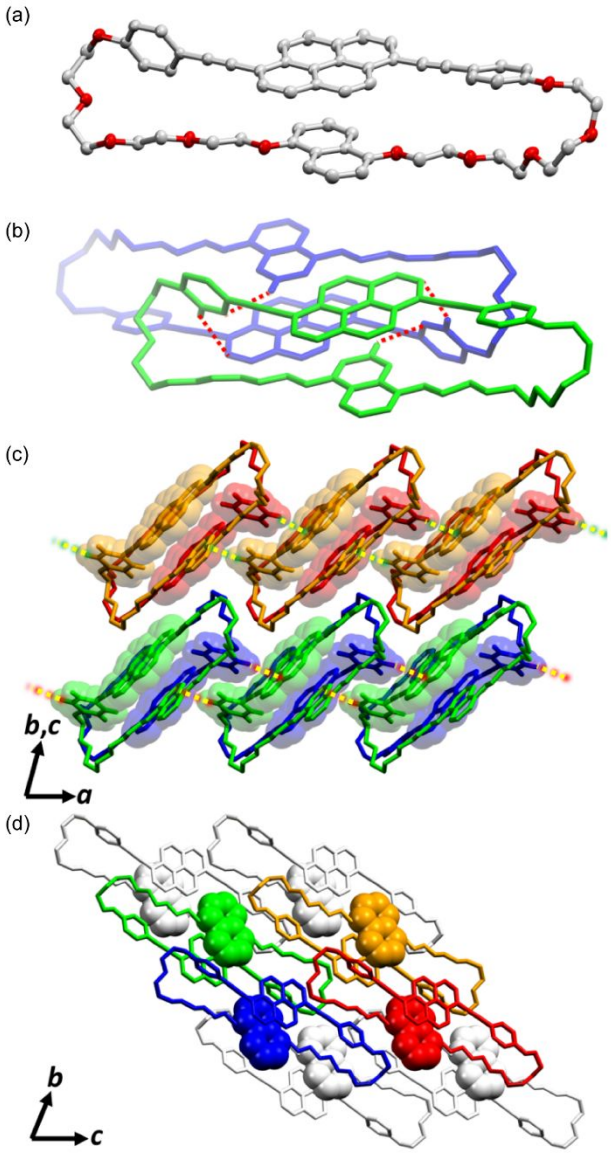


**Fig. 3** Crystal structure of cyclophane **1**. The model in (a) is a thermal ellipsoid model with 50% probability, and the others are a combination of stick and space filling models. Hydrogen atoms are omitted for clarity except ones involved in C-H•••π interactions. (a) Molecular structure of **1**. Carbon and oxygen atoms are shown in grey and red, respectively. The phenylene rings with angles of 74.12 and 15.20° to the pyrene ring are denoted as **phA** and **phB**, respectively. (b) Dimerised structure of **1**, due to intermolecular C-H•••π interactions (red dotted lines). (c) Arrangement of **1** dimers (the pairs of red-orange and blue-green molecules) in the plane parallel to (010) plane. Pyrene and **phA** rings are modelled as space filling model. (d) Packing structure viewed along the *a*-axis. The colouring of **1** on the plane parallel to (010) is the same as in (c), and **1** belonging to the adjacent 2D sheet is represented in white. Naphthalene rings are shown in space filling model, others in stick model.

where the anthracene and naphthalene are orthogonally packed.[8] Fig. 3b shows the two adjacent **1** molecules in the crystal. The angle between the averaged planes of **phA** and pyrene rings in the adjacent molecule is also 74.12°, and the hydrogen (H) atom of the **phA** ring and the C atom of the

pyrene ring are in contact. The distance of 2.900 Å is the same as the sum of the van der Waals radii of the H and C atoms. In addition, the angle between the **phA** and naphthalene rings in the adjacent molecule is 72.70°, and the H atom of the naphthalene ring is in contact with the C atom of **phA** with an H•••C distance of 2.786 Å. These edge-to-face π-interactions observed between **phA**•••pyrene and naphthalene•••**phA** rings are complementary between neighbouring molecules, suggesting that **1** forms a dimer in the crystal. Fig. 3c shows the arrangement of the **1** dimers on a plane parallel to the (010) plane. Between the dimers along the *a*-axis direction, the H atom of **phA** is also in contact with the C atoms of the pyrene rings with an H•••C distance of 2.758 Å and interplanar angle of 74.10°, indicating the C-H•••π interaction between the dimer structures. Intra-dimer and interdimer C-H•••π interactions are elongated in the *a*-axis direction through **phA** and pyrene stacking. Consequently, **1** is stacked one-dimensionally along the *a*-axis via C-H•••π interactions (Fig. 3c). The one-dimensional (1D) stacking of **1** is aligned parallel to adjacent 1D stacks in the *c*-axis direction so that their alkoxy chains interlock with each other, forming a 2D sheet structure on a plane parallel to the (010) plane. Fig. 3d shows the packing structure viewed along the *a*-axis. The C atom in the naphthalene ring and the H atom in the alkoxy chain are in contact with each other below the sum of the van der Waals radii between adjacent 2D sheets. The 2D sheets interdigitated with each other to fill the voids of each 2D sheet, forming a three-dimensional packing structure of **1**. Since the π•••π interaction can be observed within the single molecule of **1** but not between the molecules, we can consider that the π system is isolated in the packing.

**Phase transition behaviour of 1**

Next, the mechanochromic luminescence of cyclophane **1** was investigated (Fig. 4). The crystalline powder of **1** exhibits light-blue fluorescence (LB-form, $\Phi$ = 0.19). When mechanically ground, a phase transition from crystalline LB-form to green emissive amorphous phase (G-form, $\Phi$ = 0.38) occurs (see below). The initial LB-form is recovered from the G-form by annealing at 140 °C for only 1 min. The transition is provided without melting into the isotropic state. The G-form is retained for at least 1 d at r.t.

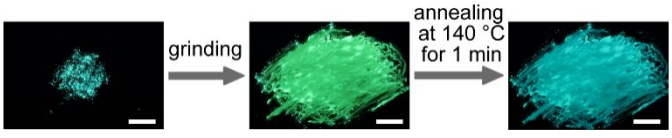


**Fig. 4** Mechanochromic luminescence of cyclophane **1**. All images were taken under 365 nm excitation light at r.t. Scale bar: 5 mm.

X-ray diffraction measurements were performed to investigate the mechanical stimuli-induced phase transition from the LB-form to the G-form and the subsequent recovery described above. The LB-form presents many peaks on the diffractogram, reflecting its crystalline nature (Fig. 5a). The experimental powder X-ray diffraction pattern is similar to the calculated diffractogram (Fig. S2) from the crystal structure shown in Fig. 3; the peak positions are slightly shifted due to thermal contraction since the single-crystal X-ray analysis was performed at –100 °C. In contrast, no clear peaks are evident in the diffraction pattern obtained for the G-form, although one ambiguous broad peak was observed around 16.5° (Fig. 5b). The diffraction patterns clearly show that the light-blue to green emission colour change is a direct result of a phase transition from crystalline to amorphous. The crystalline peaks are again evident in the diffractogram exhibited by the annealed G-form (Fig. 5c). The peak positions are almost identical to those provided for the LB-form, indicating that the initial LB-form was recovered by the annealing procedure.

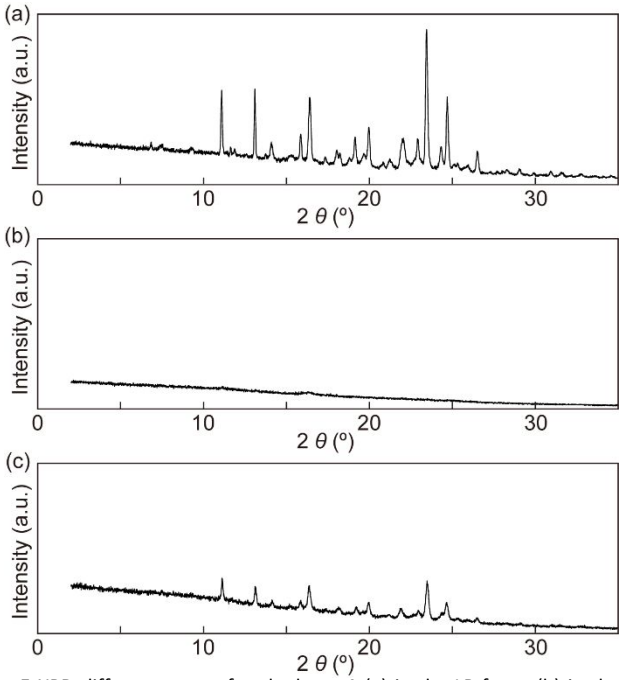


**Fig. 5** XRD diffractograms of cyclophane **1** (a) in the LB-form, (b) in the G-form, and (c) after thermal treatment for the G-form at 140 °C for 1 min. All diffractograms were recorded at r.t.

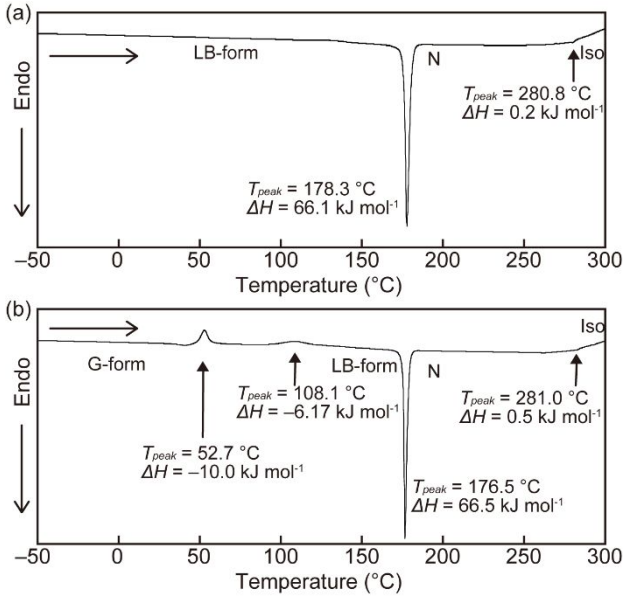

**Fig. 6** DSC curves of cyclophane **1** (a) in the LB-form and (b) in the G-form. The curves were recorded on the 1st heating. The scanning rate was 10 °C $min^{-1}$.

Differential scanning calorimetry (DSC) was conducted for both LB- and G-forms. A sharp peak was observed at 178.3 °C on the DSC trace of the LB-form upon heating (Fig. 6a). The endothermic peak is due to the transition from the crystalline phase to the LC phase. Upon further heating, compound **1** shows a transition to an isotropic state at 280.8 °C. Once the isotropic state appears, decomposition of **1** gradually occurs, which was confirmed by polarised optical microscopy (POM) observation. We characterised the LC phase as a nematic phase because a typical schlieren texture was observed by POM observation (Fig. 7). In addition, the transition enthalpy of the peak at the transparent point was significantly small ($\Delta H$ = 0.2 kJ $mol^{-1}$). Longer oligo(ethylene)glycol linkers expand liquid crystallinity as cyclophane **2** shows a phase transition from crystalline to nematic LC at 106.9 °C.[9] The DSC curve recorded for the G-form (Fig. 6b) supported the thermal stimuli-induced recovery of the LB-form. Two peaks were observed at 52.7 and 108.1 °C upon heating. The LB-form is recovered above these temperatures. As the two peaks are exothermic, the G-form appears thermodynamically metastable relative to the LB-form. Upon further heating, two endothermic peaks, as already observed in the DSC curve obtained for the LB-form, were again observed.

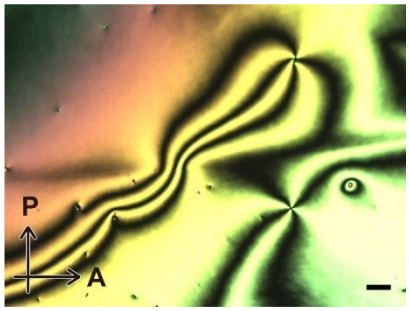


**Fig. 7** POM image of cyclophane **1** in the nematic phase at 200 °C. The image was taken in the absence of coverslip. The scale bar is 25 µm.

**Photophysical properties in solutions**

The photophysical properties of cyclophane **1** as the monomer were examined in $CHCl_3$ ($c$ = 1.0 × $10^{-5}$ M) before the mechanoresponsive behaviour was investigated in the solid states. Compounds **1**, **2**, and **3** in $CHCl_3$ displayed similar absorption bands between 350 and 450 nm (Fig. 8a). Closer inspection revealed that the spectral shapes were slightly different from each other. The $CHCl_3$ solution of **1** shows two peaks at 408 and 430 nm with molar extinction coefficients of 6.0 × $10^4$ and 6.5 × $10^4$ L $mol^{-1}$ $cm^{-1}$, respectively. In contrast, no clear peaks were observed in the absorption bands of $CHCl_3$ solutions of **2** and **3**. Furthermore, the absorption band of **1** in $CHCl_3$ was slightly redshifted compared to that of compound **3**. These differences were caused by the smaller cyclic structure of **1**. The naphthalene group restricts the free rotation of the central pyrene moiety relative to the outer phenylene groups, leading to a decrease in the number of conformations of the luminophore. Consequently, a clear vibronic structure appeared in the absorption spectrum. In addition, an enhanced proportion of the planar conformation of the luminophore resulted in a redshift of the absorption band. The naphthalene groups of cyclophanes **1** and **2** resulted in an incremental effect on the absorbance between 250 and 330 nm. Concerning the photoluminescence properties, as shown in Fig. 8b, all compounds in $CHCl_3$ showed well-dissolved vibronic structures in their fluorescence spectra. In the case of reference compound **3**, two fluorescence peaks at 440 and 467 nm and one shoulder around 500 nm were observed. The fluorescence spectrum of **1** in $CHCl_3$ was slightly redshifted, with peaks at 445 and 470 nm. The fluorescence spectra of cyclophanes **1** and **2** were almost identical. The fluorescence quantum yields of **1**, **2**, and **3** in $CHCl_3$ were 0.93, 0.95, and 0.97, respectively.

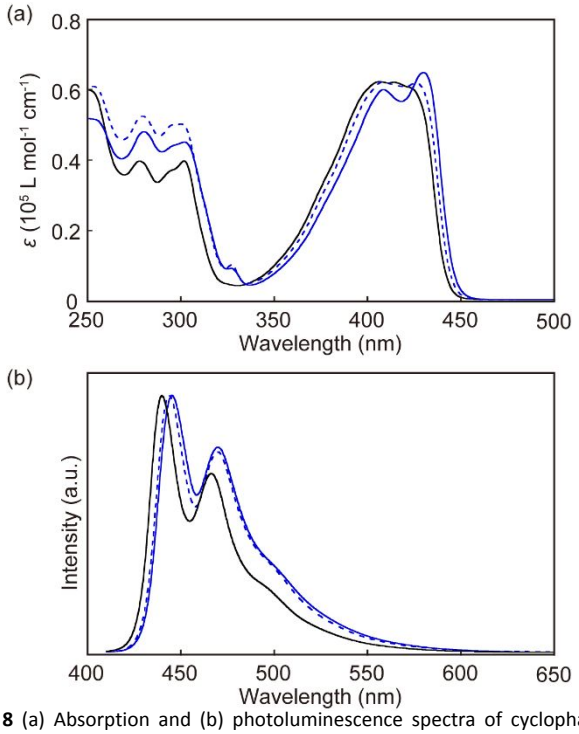


**Fig. 8** (a) Absorption and (b) photoluminescence spectra of cyclophane **1** (blue solid line), cyclophane **2** (blue dotted line), and reference compound **3** (black line) in $CHCl_3$ ($c$ = 1.0 × $10^{-5}$ M). All spectra were recorded at r.t. with $\lambda_{ex}$ value of 400 nm.

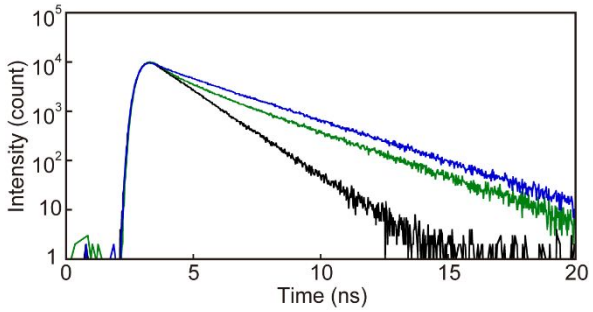


**Fig. 9** Emission decay profiles recorded for compounds **1** (blue line), **2** (green

line), and **3** (black line) in $CHCl_3$ ($c$ = 1.0 × $10^{-6}$ M). All curves were monitored at 450 nm with an excitation light of 405 nm.

The cyclic structure also affects the fluorescence lifetime of the luminophore. Fig. 9 shows the emission decay profiles of diluted $CHCl_3$ solutions of compounds **1**, **2**, and **3**. The decay profile recorded for **3** in $CHCl_3$ was well fitted with a single exponential decay function, and a monomer emission lifetime of 1.2 ns was calculated. The calculated radiative and non-radiative rate constants for **3** in $CHCl_3$ were 8.0 × $10^8$ $s^{-1}$ and 0.3 × $10^8$ $s^{-1}$, respectively. Cyclophanes **1** and **2** display decay curves that are different from that of reference compound **3**. Both curves indicated longer emission lifetime components and could be fitted with biexponential decay functions. As the result, emission lifetimes of 2.6 and 2.3 ns were obtained from the decays of cyclophanes **1** and **2**, respectively, which are also corresponding to monomers and become longer than the monomer emission lifetime of acyclic compound **3**. The incremental effect would be ascribed to decreases in radiative rate constants of the luminophore, though the rates cannot be quantitatively obtained due to the two emission species. The increases in emission lifetime are also attributed to the cyclic structure that limits the rotation and vibration of the luminophore, leading to the suppression of the radiation-less decay process from the singlet excited state. Shorter emission lifetimes of 0.5 and 0.6 ns were also obtained from the decay profiles of cyclophanes **1** and **2**, respectively. We assumed that the ground state electronic interaction between the luminophore and naphthalene group can result in emission spices with shorter emission lifetimes.

**Photophysical properties in the solid state**

The photoluminescence spectra of **1** in the solid state were measured to investigate the mechanochromic luminescence of **1**. The LB-form displays a peak at 489 nm and two shoulders at approximately 475 and 525 nm (Fig. 10, blue solid line). After grinding, the G-form presents a redshifted emission spectrum with a peak at 529 nm (Fig. 10, green line). In addition, the spectral shape is broad and structureless, suggesting that excimer formation of the luminophores occurred. This is supported by the fact that several 1,6-bis(phenylethynyl)pyrene derivatives form excimers in the molecular assembled states and their emission spectra are also broad and structureless.[9,10,68] This type of excimer is referred to as “static excimer” where the luminophores are pre-associated, which is different from “dynamic excimer” well observed in solutions.[71] As shown in the crystal structure shown in Fig. 3, the luminophores provide no clear π-π overlap. Therefore, no excimer emission was observed in the LB-form. In contrast, grinding disturbs the crystal structure and causes excimer formation. The photoluminescence spectrum shows a blueshift upon thermal treatment (Fig. 10, blue dotted line). New peaks were observed at 467 and 484 nm, and one shoulder appears at approximately 525 nm. The difference in spectral shape between the LB-form and the annealed G-form is caused by the self-absorption effect, because the ground samples become significantly thinner.

To obtain more insight into the colour changing behaviour of cyclophane **1**, emission lifetime measurements were performed for the LB-, G-, and annealed G-forms. The decay curve recorded for the G-form was fitted with a multi-exponential decay function, and a longer lifetime of 19 ns was observed. The emission species with the longer lifetime supports the mechanical stimuli-induced excimer formation in the G-form. Similar long emission lifetimes have been found for other 1,6-bis(phenylethynyl)pyrene derivatives and characterised as excimers.[9,10,60] The decay profiles of the initial LB-form and annealed G-form are different from that of the G-form. Indeed, shorter emission lifetimes were calculated from the decay profiles. The similarity between the two decays indicated that the luminophore arrangement in the LB-form is recovered by a combination of grinding and subsequent thermal treatment.

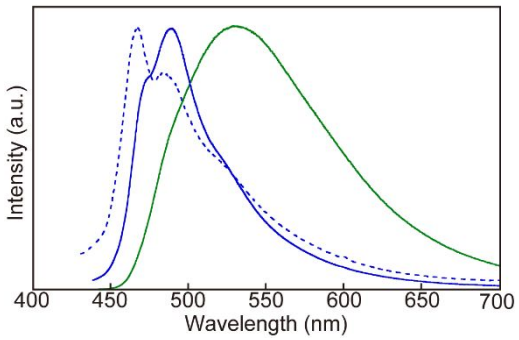


**Fig. 10** Photoluminescence spectra of cyclophane **1** in the LB-form (blue line), in the G-form (green line), and in the sample after thermal treatment for the G-form (blue dotted line). All spectra were recorded at r.t. with an excitation light of 400 nm.

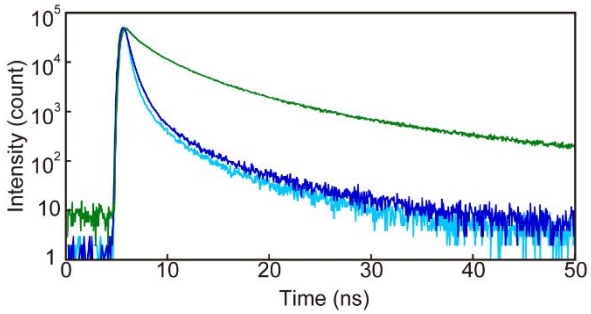


**Fig. 11** Emission decay profiles recorded for compound **1** in the LB-form (monitored at 480 nm, blue line), in the G-form (monitored at 530 nm, green line), and in the annealed G-form (monitored at 480 nm, light blue line). All curves were monitored with an excitation light of 405 nm.

## Conclusions

In summary, the crystal structures of 1,6-bis(phenylethynyl)pyrene-based cyclophane **1** was solved, and the mechanochromic luminescence was demonstrated. The moderate length of the linkers between two aromatic groups allows us to access single crystals in which the pyrene and naphthalene moieties form an intramolecular π–π stacked structure. Two cyclophane molecules form dimers through complementary intermolecular edge-to-face π-interactions.

The dimers are arranged three-dimensionally to form a crystalline LB-form. π–π interactions do not occur among the luminophores in the LB-form, thus eliminating excimer emission. Once mechanically ground, the phase transition occurs from the crystalline LB-form to the amorphous G-form, in which a part of the luminophores form excimers, leading to an emission colour change from light-blue to green. The initial LB-form is recovered by annealing the G-form at 140 °C for 1 min.

Estimating the molecular arrangement of the cyclophanes in the solid state is inherently challenging because of their flexible and cyclic structure. Therefore, solving the crystal structure plays a pivotal role in investigating the mechano- and/or thermochromic luminescence of cyclophanes. Trials to obtain single crystals of cyclophane with other luminophores are currently being conducted by our group.

## Conflicts of interest

There are no conflicts to declare.

## Acknowledgements

We thank the Open Facility Center, Tokyo Institute of Technology, for powder X-ray diffraction measurements and elemental analysis. This work was supported by JSPS KAKENHI (grant no. JP18H02024, JP18H01949, JP20H05198, and JP21K14691). This work was also supported by the Suematsu Challenging Research Award. This work was supported in part by Japan Science Technology Agency (JST), FOREST (Grant JPMJFR201N).

## Notes and references

1. Y. Sagara, S. Yamane, M. Mitani, C. Weder and T. Kato, *Adv. Mater.*, 2016, **28**, 1073–1095.
2. Y. Sagara and T. Kato, *Nat. Chem.*, 2009, **1**, 605–610.
3. Z. Chi, X. Zhang, B. Xu, X. Zhou, C. Ma, Y. Zhang, S. Liu and J. Xu, *Chem. Soc. Rev.*, 2012, **41**, 3878–3896.
4. X. Zhang, Z. Chi, Y. Zhang, S. Liu and J. Xu, *J. Mater. Chem. C*, 2013, **1**, 3376–3390.
5. Z. Ma, Z. Wang, M. Teng, Z. Xu and X. Jia, *ChemPhysChem*, 2015, **16**, 1811–1828.
6. S.-N. Lei, H. Xiao, Y. Zeng, C.-H. Tung, L.-Z. Wu and H. Cong, *Angew. Chem. Int. Ed.*, 2020, **59**, 10059–10065.
7. S. Izumi, H. F. Higginbotham, A. Nyga, P. Stachelek, N. Tohnai, P. d. Silva, P. Data, Y. Takeda and S. Minakata, *J. Am. Chem. Soc.*, 2020, **142**, 1482–1491.
8. Y. Sagara, K. Takahashi, A. Seki, T. Muramatsu, T. Nakamura and N. Tamaoki, *J. Mater. Chem. C*, 2021, **9**, 1671–1677.
9. Y. Sagara, C. Weder and N. Tamaoki, *Chem. Mater.*, 2017, **29**, 6145–6152.
10. Y. Sagara and N. Tamaoki, *RSC Adv.*, 2017, **7**, 47056–47062.
11. Y. Sagara, Y. C. Simon, N. Tamaoki and C. Weder, *Chem. Commun.*, 2016, **52**, 5694–5697.
12. P. G. Ghasemabadi, T. Yao and G. J. Bodwell, *Chem. Soc. Rev.*, 2015, **44**, 6494–6518.
13. C. J. Brown and A. C. Farthing, *Nature*, 1949, **164**, 915–916.
14. D. J. Cram and H. Steinberg, *J. Am. Chem. Soc.*, 1951, **73**, 5691–5704.
15. D. J. cram and J. M. Cram, *Acc. Chem. Res.*, 1971, **4**, 204–213.
16. C. Seel and F. Vögtle, *Angew. Chem. Int. Ed.*, 1992, **31**, 528–549.
17. A. Jasat and J. C. Sherman, *Chem. Rev.*, 1999, **99**, 931–968.
18. J. O. Jeppesen, M. B. Nielsen and J. Becher, *Chem. Rev.*, 2004, **104**, 5115–5132.
19. P. P. Neelakandan, K. S. Sanju and D. Ramaiah, *Photochem. Photobiol.*, 2010, **86**, 282–289.
20. M. Xue, Y. Yang, X. Chi, Z. Zhang, and F. Huang, *Acc. Chem. Res.*, 2012, **45**, 1294–1308.
21. A. M. Agafontsev, T. A. Shumilova, T. Rüffer, H. Lang, and E. A. Kataev, *Chem. Eur. J.*, 2019, **25**, 3541–3549.
22. W. Wang, L. Wang, B. J. Palmer, G. J. Exarhos and A. D. Q. Li, *J. Am. Chem. Soc.*, 2006, **128**, 11150–11159.
23. J. F. Stoddart, *Chem. Soc. Rev.*, 2009, **38**, 1802–1820.
24. R. S. Forgan, J.-P. Sauvage and J. F. Stoddart, *Chem. Rev.*, 2011, **111**, 5434–5464.
25. A. C. Fahrenbach, C. J. Bruns, D. Cao and J. F. Stoddart, *Acc. Chem. Res.*, 2012, **45**, 1581–1592.
26. S. F. M. van Dongen, S. Cantekin, J. A. A. W. Elemans, A. E. Rowan and R. J. M. Nolte, *Chem. Soc. Rev.*, 2014, **43**, 99–122.
27. J. F. Stoddart, *Angew. Chem. Int. Ed.*, 2014, **53**, 11102–11104.
28. C. J. Bruns and J. F. Stoddart, *Acc. Chem. Res.*, 2014, **47**, 2186–2199.
29. G. Gil-Ramírez, D. A. Leigh and A. J. Stephens, *Angew. Chem. Int. Ed.*, 2015, **54**, 6110–6150.
30. S. Erbas-Cakmak, D. A. Leigh, C. T. McTernan and A. L. Nussbaumer, *Chem. Rev.*, 2015, **115**, 10081–10206.
31. Y. Sagara, M. Karman, E. Verde-Sesto, K. Matsuo, Y. Kim, N. Tamaoki and C. Weder, *J. Am. Chem. Soc.*, 2018, **140**, 1584–1587.
32. Y. Sagara, M. Karman, A. Seki, M. Pannipara, N. Tamaoki and C. Weder, *ACS Cent. Sci.*, 2019, **5**, 874–881.
33. T. Muramatsu, Y. Sagara, H. Traeger, N. Tamaoki and C. Weder, *ACS Appl. Mater. Interfaces*, 2019, **11**, 24571–24576.
34. T. Muramatsu, Y. Okado, H. Traeger, S. Schrettl, N. Tamaoki, C. Weder and Y. Sagara, *J. Am. Chem. Soc.*, 2021, **143**, 9884–9892.
35. P. R. Ashton, D. Joachimi, N. Spencer, J. F. Stoddart, C. Tschierske, A. J. P. White, D. J. Williams and K. Zab, *Angew. Chem. Int. Ed.*, 1994, **33**, 1503–1506.
36. V. Percec, A. D. Asandei and P. Chu, *Macromolecules*, 1996, **29**, 3736–3750.
37. V. Percec, A. D. Asandei and G. Ungar, *Chem. Mater.*, 1996, **8**, 1550–1557.
38. V. Percec, P. J. Turkaly and A. D. Asandei, *Macromolecules*, 1997, **30**, 943–952.
39. B. Neumann, D. Joachimi and C. Tschierske, *Adv. Mater.*, 1997, **9**, 241–244.
40. B. Neumann, T. Hegmann, C. Wagner, P. R. Ashton, R.

Wolf and C. Tschierske, *J. Mater. Chem.*, 2003, **13**, 778–784.
41. T. Hegmann, B. Neumann, R. Wolf and C. Tschierske, *J. Mater. Chem.*, 2005, **15**, 1025–1034.
42. K. Nabeya, T. Muraoka, N. Hoshino, M. Aizawa, T. Kajitani, T. Akutagawa, A. Shishido, T. Fukushima and K. Kinbara, *Mater. Chem. Front.*, 2018, **2**, 969–974.
43. H. Langhals and R. Ismael, *Eur. J. Org. Chem.*, 1998, **1998**, 1915–1917.
44. J. Feng, Y. Zhang, C. Zhao, R. Li, W. Xu, X. Li and J. Jiang, *Chem. Eur. J.*, 2008, **14**, 7000–7010.
45. S. Liu, D. Schmitz, S.-S. Jester, N. J. Borys, S. Hoger and J. M. Lupton, *J. Phys. Chem. B*, 2013, **117**, 4197–4203.
46. K. E. Brown, W. A. Salamant, L. E. Shoer, R. M. Young and M. R. Wasielewski, *J. Phys. Chem. Lett.*, 2014, **5**, 2588–2593.
47. A. Garci, Y. Beldjoudi, M. S. Kodaimati, J. E. Hornick, M. T. Nguyen, M. M. Cetin, C. L. Stern, I. Roy, E. A. Weiss and J. F. Stoddart, *J. Am. Chem. Soc.*, 2020, **142**, 7956–7967.
48. I. Roy, S. Bobbala, J. Zhou, M. T. Nguyen, S. K. M. Nalluri, Y. Wu, D. P. Ferris, E. A. Scott, M. R. Wasielewski and J. F. Stoddart, *J. Am. Chem. Soc.*, 2018, **140**, 7206–7212.
49. M.-P. Teulade-Fichou, J.-P. Vigneron and J.-M. Lehn, *J. Chem. Soc., Perkin Trans. 2*, 1996, 2169–2175
50. O. Baudoin, F. Gonnet, M.-P. Teulade-Fichou, J.-P. Vigneron, J.-C. Tabet and J.-M. Lehn, *Chem. Eur. J.*, 1999, **5**, 2762–2771.
51. M. Inouye, K. Fujimoto, M. Furusyo and H. Nakazumi, *J. Am. Chem. Soc.*, 1999, **121**, 1452–1458.
52. H. Abe, Y. Mawatari, H. Teraoka, K. Fujimoto and M. Inouye, *J. Org. Chem.*, 2004, **69**, 495–504.
53. P. P. Neelakandan and D. Ramaiah, *Angew. Chem. Int. Ed.*, 2008, **47**, 8407–8411.
54. D. Ramaiah, P. P. Neelakandan, A. K. Nair and R. R. Avirah, *Chem. Soc. Rev.*, 2010, **39**, 4158–4168.
55. L. Qiu, C. Zhu, H. Chen, M. Hu, W. He and Z. Guo, *Chem. Commun.*, 2014, **50**, 4631–4634.
56. P. Spenst and F. Würthner, *Angew. Chem. Int. Ed.*, 2015, **54**, 10165–10168.
57. P. C. Nandajan, P. P. Neelakandan and D. Ramaiah, *RSC Adv.*, 2013, **3**, 5624.
58. J. Yang, C.-C. Dong, X.-L. Chen, X. Sun, J.-Y. Wei, J.-F. Xiang, J. L. Sessler and H.-Y. Gong, *J. Am. Chem. Soc.*, 2019, **141**, 4597–4612.
59. Y. Sagara, K. Takahashi, T. Nakamura and N. Tamaoki, *Mol. Syst. Des. Eng.*, 2020, **5**, 205–211.
60. Y. Sagara, H. Traeger, J. Li, Y. Okado, S. Schrettl, N. Tamaoki and C. Weder, *J. Am. Chem. Soc.*, 2021, **143**, 5519–5525.
61. K. Mase, Y. Sasaki, Y. Sagara, N. Tamaoki, C. Weder, N. Yanai and N. Kimizuka, *Angew. Chem. Int. Ed.*, 2018, **57**, 2806–2810.
62. Y. Sagara, N. Tamaoki and G. Fukuhara, *ChemPhotoChem*, 2018, **2**, 959–963.
63. Y. Sagara, A. Seki, Y. Kim and N. Tamaoki, *J. Mater. Chem. C*, 2018, **6**, 8453–8459.
64. H. Maeda, T. Maeda, K. Mizuno, K. Fujimoto, H. Shimizu and M. Inouye, *Chem. Eur. J.*, 2006, **12**, 824–831.
65. C. V. Suneesh and K. R. Gopidas, *J. Phys. Chem. C*, 2010, **114**, 18725–18734.
66. J. Xiao, J. Xu, S. Cui, H. Liu, S. Wang and Y. Li, *Org. Lett.*, 2008, **10**, 645–648.
67. S. Diring, F. Camerel, B. Donnio, T. Dintzer, S. Toffanin, R. Capelli, M. Muccini and R. Ziessel, *J. Am. Chem. Soc.*, 2009, **131**, 18177–18185.
68. A. Yoshizawa and M. Inouye, *ChemPhotoChem*, 2018, **2**, 353–356.
69. Y. Sagara and T. Kato, *Angew. Chem. Int. Ed.*, 2008, **47**, 5175–5178.
70. Y. Sagara, T. Komatsu, T. Ueno, K. Hanaoka, T. Kato and T. Nagano, *J. Am. Chem. Soc.*, 2014, **136**, 4273–4280.
71. F. M. Winnik, *Chem. Rev.*, 1993, **93**, 587–614.